

Assistive Robotic Grasping

Jonathan D. Weisz

Submitted in partial fulfillment of the
requirements for the degree
of Doctor of Philosophy
in the Graduate School of Arts and Sciences

COLUMBIA UNIVERSITY

2015

©2015

Jonathan D. Weisz

All Rights Reserved

ABSTRACT

Assistive Robotic Grasping

Jonathan D. Weisz

This thesis describes some contributions towards the implementation of Human-in-the-Loop(HitL) grasping for assistive robotics, with a particular focus on low throughput, high noise interfaces such as electroencephalography(EEG) or electromyography(EMG) brain-computer interface(BCI) devices in natural environments. Although progress in the robotics field has been swift, it is unlikely that truly independent operation of robots in situations where they will interact closely with objects, obstacles, and perhaps even other people in their environment will evolve in the immediate future. However, with the help of a human operator, it is possible to achieve robust, safe operation in complex environments. This work describes a system that can accomplish this with minimal interfaces that are accessible even to individuals with impairments, which will enable the development of more capable assistive devices for these individuals.

Grasping an object generally requires contextual knowledge of the object and the intent of the user. We have developed a user interface for an on-line grasp planner that allows the user to effectively express their intent. Grasping in natural environments requires grasp planning algorithms that are robust to target localization errors. This work describes grasp quality measurements that generate more robust grasps by considering the local geometry of the object as well as how uncertainty will effect the proposed grasp. These new measures are integrated into an augmented reality interface that allows a user to plan a grasp online that matches their intent for using the object that is to be grasped. This interface is validated by testing with real users, both healthy and impaired, using a variety of input devices suitable for impaired subjects, such as low cost EEG and EMG devices. This work forms the foundation for a flexible, fully featured HitL system that will allow users to grasp objects in cluttered spaces using novel, practical BCI devices that have the potential to

bring HiTL assistive devices out of the research environment and into the lives of those that need them.

Table of Contents

1	Introduction	1
1.1	The Promise of Assistive Robotics	1
1.2	The Challenge of Robotic Grasping	2
1.3	The Eigengrasp Planner	2
1.4	An Integrated Assistive Robotic Grasping Platform	3
1.5	The Contribution Of This Thesis	4
2	Related Work	6
2.1	Brain Computer Interfaces with Robotics	6
2.1.1	Overview	6
2.1.2	Direct Demonstration	7
2.1.3	Joint Level Control	7
2.1.4	End Effector Cartesian Control	8
2.1.5	Discrete Mode Control	9
2.1.6	Task Level Control	10
2.2	Robust Grasping	10
2.2.1	Wrench Space Metrics	11
2.2.2	Wrench Space Metrics Robust to Contact Location Uncertainty . . .	11
2.2.3	Simplified Analytical models of Robustness	12
2.2.4	Sampling Based Heuristics	12
3	Robust Grasping	14
3.1	Grasp Planning with Contact Points	14

3.2	Grasp Wrench Spaces	15
3.3	The ϵ_{GWS} Quality Metric	16
3.4	Optimization Based Grasp Planning	16
3.4.1	Potential Contact Quality Function	17
3.4.2	Implications for pose error robustness	17
3.5	Analyzing The Effects of Pose Error In Simulation	18
3.5.1	The Columbia Grasp Database	18
3.5.2	Grasping Pipeline	19
3.5.3	Model of Pose Uncertainty	20
3.5.4	Simulation Results	21
3.5.5	Chosing optimal grasps: ϵ_{GWS} vs $P(fc)$	23
3.6	Physical Experiments	24
3.7	Discussion	29
3.7.1	Online Extensions	29
I	Bibliography	31
	Bibliography	32

List of Figures

3.1	An example of a grasp where the ϵ_{GWS} is consistent with respect to the common localization errors, and one where it is not.	17
3.2	<i>Illustration of the initial pose and posture.</i> The hand is withdrawn along its approach direction and all of the fingers opened at the same constant velocity until each of the fingertips are outside of the knuckles of the hand in its pre-grasp configuration. The hand is then opened an additional ten percent of the remaining joint range. The pre-grasp configuration is shown in green. .	20
3.3	Illustration of the tabletop error model used in this paper. The object is can be translated $[-10, 10]$ mm in both X and Y and rotated $[-20, 20]^\circ$ around θ . The red cones mark the planned contact points. The white wire frame indicates the planned end configuration of the fingers.	21
3.4	ϵ_{GWS} plotted against $P(fc)$, which is equivalent to the probability of attaining a force closed grasp under our error model from a planned starting grasp configuration. 480 grasps over 96 objects are presented in this figure. This figure demonstrates that the ϵ_{GWS} is generally a poor predictor of pose error robustness as measured by the $P(fc)$. The mean ϵ_{GWS} , denoted by the black line, is 0.095. There appears to be a cutoff, denoted by a red vertical line on the graph, around $\epsilon_{GWS} > 0.2$, after which all available grasps are have a high $P(fc)$, but note how few grasps there are in the database with quality values that high. Only five objects have a grasp with a quality that high, which implies that for most objects, ϵ_{GWS} cannot be used to predict $P(fc)$.	25

3.5	<i>Results A:</i> The results of physical experiments on five large, complex objects. In the left column are the best grasps for each object ranked by ϵ_{GWS} . An example of the simulated and physically realized grasp is illustrated for each grasp attempted. Additionally, the figure gives the $P(fc)$ and ϵ_{GWS} for each grasp attempted, as well as the fraction of attempts which succeeded in lifting the object by 3 cm in physical experiments. The higher $P(fc)$ grasp is successful on many more trials than the higher ϵ_{GWS} grasp for these objects.	27
3.6	<i>Results B:</i> The results of physical experiments on five smaller, simpler objects. In the left column are the best grasps for each object ranked by ϵ_{GWS} . In the right column are the best grasps by $P(fc)$. An example of the simulated and physically realized grasp is illustrated for each grasp attempted. Additionally, the figure gives the $P(fc)$ and ϵ_{GWS} for each grasp attempted, as well as the fraction of attempts which succeeded in lifting the object by 3 cm in physical experiments.	28

List of Tables

3.1	Summary of Simulation Results: These results quantify how robust each quality measure is to pose uncertainty. For each grasp, the expected value and standard deviation of the respective quality measures are calculated across the poses sampled. These measures are normalized by dividing them by the planned quality of the unperturbed grasp to allow comparison of the effects of uncertainty across grasps. $P(fc)$ denotes the measured probability of achieving a force closed grasp, which we have calculated as $P(\epsilon_{GWS} > .001)$	23
3.2	This table quantifies the effect of sampling parameters on the estimate of quality measure. The first column describes the sampling density along each dimension of the error model. The other columns describe the average change in the subsampled $P(fc)$ as compared to the densest sampling rate. This demonstrates that	30

Acknowledgments

The acknowledgments go here. The acknowledgments go here.

Dedication text

Chapter 1

Introduction

1.1 The Promise of Assistive Robotics

Although progress in the robotics field has been swift, it is unlikely that truly independent operation of robots in situations where they will interact closely with objects, obstacles, and perhaps even other people in their environment will evolve in the immediate future. However, with the help of a human operator, it is possible to achieve robust, safe operation in complex environments. This work describes a system that can accomplish this with minimal interfaces that are accessible even to individuals with impairments, which will enable the development of more capable assistive devices for these individuals.

Grasping is important for many activities of daily living (ADL) that physically impaired individuals need assistance performing, such as fetching food or communication devices. There is a large and growing population with upper limb mobility issues in the United States. There are currently 400,000 individuals with spinal cord injuries, 50% of whom suffer upper limb mobility issues, 5 million individuals that have suffered from strokes, and a generally aging worldwide population. This presents an urgent need for better assistive technologies. The individuals with the greatest need for assistive technologies are those with severe impairments. By the nature of their health challenges, they are often limited in their ability to provide input to an assistive device. To address this concern, there has been a great deal of interest in Brain Computer Interface (BCI) devices over the last few years. In general, these devices are restricted to low bandwidth, noisy signals. Therefore, using these

devices to control an assistive device poses many challenges.

1.2 The Challenge of Robotic Grasping

Irrespective of the problems of BCI interface, robotic grasping is challenging for a number of reasons. First, complex robotic hands have many degrees of freedom, which makes the space of possible grasps extremely difficult to explore. Standard approaches to planning in high dimensional state spaces are likely to fail with many fingered hands, especially as the grasp itself involves purposeful collision with the object, but most of the "near grasp" states will be overlapping the object in some way. Secondly, evaluating grasps involves several properties that are difficult to model, such as friction and closed chain kinematics. Many analysis tools that currently the state of the art are only effective if the contact points can be perfectly predicted and the grasp acquisition can be perfectly controlled so that the object is not moved. Finally, robotic hands are extremely heterogeneous in terms of their physical size, the arrangement of their sensors, and their actuators, which makes finding generic strategies difficult.

In addition to all of these issues, in natural environments, any set of grasps that is preplanned may overlap with obstacles in the environment or fail to grasp the object in a way that is well suited to the desired use of the object, so grasp planning algorithms must be fast enough to run online, and be able to reflect the intent of the use of the grasp beyond simple stability. Until these challenges are overcome, robots will remain of limited utility as helpers for improving the lives of people outside of the lab.

1.3 The Eigengrasp Planner

Previous work in our lab by Ciocarlie et al. has attempted to address the main challenges of grasp planning by producing the Eigengrasp Planner. The planner addresses these issues by following a dimensionality reduction strategy that reduces the state space of the hand so that a sampling based stochastic optimization strategy can be used with a relatively simple grasp quality metric. The quality metric that is used by the planner evaluates a projection of the fingers on to the target object, which makes the state space easier to evaluate because

the quality function is valid in configurations where the hand is not in contact with the object. The nature of the optimization approach, which gradually moves towards lower values of the quality function, should produce solutions where nearby finger contacts will also provide similar quality grasps because grasps where nearby points are poor will have narrow basins of attraction that are less likely to be found. This implies a certain amount of robustness to the small displacements of the object during grasp acquisition. The planner is easy to generalize because the only robot specific parameters are the state space reduction strategy and a set of desirable contact locations, which can be easily specified for any given robot.

The planner is fast enough to run in near real time, and can be made responsive to user intent by biasing the search of the stochastic optimization towards a pose that is demonstrated by a human operator. In this model, the desired intent of the user is indicated by demonstrating a desired direction and approximate location to grasp from, possibly by moving a virtual hand in a simulated environment.

The efficacy of Eigengrasp Planner's approach was validated demonstrated by having an operator hold a robotic hand's base and move it around a target object while running the planner. When the planner found a grasp that appeared reasonable, the operator would grasp the object by simply clicking a single key. The approach of the hand to the object and the application of force to the hand as it contacted the object were controlled manually by the operator. This demonstration was extremely compelling, and the problem appeared to be largely solved. However, some limitations of this approach were exposed in attempting to translate this work from the initial demonstration to a platform that could be used by a disabled person, given the limitations of the input devices available.

1.4 An Integrated Assistive Robotic Grasping Platform

To begin addressing even the most basic needs of an impaired individual with assistive robotics technologies, we need an underlying platform for robust grasping. Such a system would need to integrate path planning, object localization and identification, and grasp planning with a user interface suitable for whatever signals the user is able to supply. Al-

though fully automated approaches for each of these components have been the subject of extensive and ongoing research, integrating user input to create a shared-control environment that uses as much input as the user is able to supply is still a relatively unexplored field. There are many possible paradigms for integrating BCIs with a shared-control assistive robotics device. Traditional EMG and EEG setups are expensive and difficult to deploy. Recently, cheap and portable EEG headsets have become available, and new devices such as portable near-infrared-spectroscopy (NIRS) devices and single electrode EMG devices are also reaching the market.

These devices expand the potential for a practical, multimodal BCI system that can be taken out of the laboratory and in an assistive robotics environment. Grasp planning is a difficult, unsolved problem. Online planning and grasp planning under sensor uncertainty are each independently unsolved problems that need further exploration. Putting the human in the loop when planning and executing the grasp in real time fundamentally changes the nature of the problem as compared to a fully automated system. The key part of the problem becomes conveying information to the user effectively about the state of the system and then using the low bandwidth information gained from the user efficiently. This requires us to think carefully about the interfaces provided to the user and how we infer intent from the users input. Additionally, in order to present the user with reasonable grasping options, we need to extend the existing grasp stability analyses to deal with the most common problems that arise in unstructured environments, object localization errors due to sensor noise.

1.5 The Contribution Of This Thesis

This thesis extends and refines the initial work on the eigengrasp planner to a flexible integrated assistive robotics grasping platform, and demonstrates its application to a number of different input devices designed for severely impaired individuals. Two main issues are addressed. Without the benefits of complete control over the grasping process and the assumption of perfect localization of the target object, significantly more care has to be giving to selecting robust grasps. Additionally, the user cannot be assumed to have fine control over the demonstration pose because their input device may not provide the bandwidth that

such control requires. This means we need to devise a user interface that can accomodate a more limited input

To address the first issue, I present the large scale first analysis of how the seminal grasp quality measures proposed by Ferrari and Canny is expected to vary under realistic models of object location uncertainty in ???. This analysis shows that the grasps produced by the EigenGrasp planner are not sufficiently robust under even modest location uncertainties. From this analysis, I derive an extension of the grasp quality measure that produces significantly more robust grasps.

I will present the novel platform that we have developed to apply this planner using several different brain computer interfaces. These interfaces take advantage of the fact that many severely impaired individuals who lose function in their limbs still maintain control over their facial muscles, from which we can extract a few control signals reliably. These devices are relatively low cost and noninvasive compared with most other modalities of getting signals from impaired individuals. In chapter ?? I will present the development of the integrated system, including the object localization methodology, the online grasp filtering, and further refinements to the grasp planning system to improve it's speed and quality. In chapter ??, I will describe implementation of this interface with the Emotiv Epoc, a commercial EEG/EMG device, and a combination of facial gestures and EEG control, and the results achieved by a healthy cohort of subjects. In chapter ??, I will describe an interface which uses much more minimal and practical surface EMG device that is much more easily deployable than the Epoc and other similar cap devices, because it requires only a single recording site and a few wires. We will see that an impaired individual is able to grasp objects using this minimalistic device after only a short introduction to the grasping platform. Based on these experiments, we further refined this system and present these refinements as well as a healthy cohorts capabilities with the system in chapter ??

Chapter 2

Related Work

2.1 Brain Computer Interfaces with Robotics

2.1.1 Overview

There is a long historical precedent for engineering assistive systems using electrophysiological signals to drive robotic devices [Schmidl, 1965], with a commercial version being introduced by [Sherman and Lippay, 1965] as early as 1965. In the time since, there have been myriad approaches and refinements of proposed to interfacing disabled individuals with robotic assistive systems, and this work will not review even a small fraction of them. There are two ways of categorizing these types of systems. One way is to categorize the system by the input modality; That is whether it uses physical buttons or pointing devices, some external sensor of motion such as eye or hand trackers, or some specific electrophysiological signal such as EMG, EOG, and EEG. Another consideration is where the signals are recorded from. EMG can be recorded from distal muscle sites, which may be larger, easier to record from, and produce larger signals. However, more impaired individuals tend to maintain control over muscle functions closer to the head

Another way to categorize the systems is by the type of control they engender - whether the control is at a task level, allowing the user to designate what is to be done, or at a state level, allowing the user to specify joint angles, or end effector positions.

This work presents a system at an intermediate level, in which the user has some state

level control that is task oriented. This requires an online planning system that generates robust grasps in realtime. Below I describe the different control paradigms used in related systems using BCI devices.

2.1.2 Direct Demonstration

The most intuitive, low level of control of a robotic arm involves having the robot arm directly mimic the motions of the user. It is possible to reconstruct a user's movements using surface distal limb surface EMG signals, as in [Artemiadis and Kyriakopoulos, 2011; Castellini and van der Smagt, 2009]. This type of control allows the user to express their desires explicitly, allowing the user to specify how the arm is to avoid objects. A mapping from the subjects joints to the robotic arm can be found that ensures that the robot stays approximately the same distance from it's joint limits as the subject does, which ensures that the robot's workspace will be compatible with the intent of the user in manipulating objects.

This paradigm is not suitable for assistive robotic interfaces because the impaired individuals have lost exactly the capability used as the control input to this type of interface.

2.1.3 Joint Level Control

Rather than implicitly controlling the arm, some paradigms allow the user explicit control of joints of the robot. This generally imposes a much higher cognitive load on the user, as they have to attend closely to each joint. The movement of the joints are not directly related to user's goal of manipulating some object. Control of a manipulator through such an interface is generally not possible because they have many joints. The manipulator is generally controlled by simple open and close commands. For example, in [Horki *et al.*, 2011] hand opening/closing and elbow flexion/extension are controlled by EEG signals.

For a prosthetic arm with essentially two degrees of freedom, this sort of control may be appropriate, but more degrees of freedom will strain the bit rate of these types of devices and their unreliability will make the coordination necessary to perform complex tasks in natural environments difficult or impossible. For example, to grasp an object using a six degree manipulator with a gripper, the user must in a straight line towards an object, or

the gripper will not move straight and the finger may knock over the object while moving the palm into place. This requires that the user simultaneously send coordinated signals to all six degrees in exactly the right ratios, or it may not move in anything close to a straight line.

2.1.4 End Effector Cartesian Control

The main goal of a robotic manipulator is to interact with the world with some end effector. Giving the user direct control over the end effector location can be more intuitive, because the user generally has an end effector location is the variable that the user most directly observes. These works are range in invasiveness and signal quality from using a high fidelity implanted electrode array to reconstruct the desired end effector movement, as shown by [Vogel *et al.*, 2010], to using much lower bandwidth surface electrode based systems for tracking eye movement, as in [Postelnicu *et al.*, 2011]. Several authors have proposed using various facial EMG reading systems to do achieve cartesian end effector control, such as these [[Sagawa and Kimura, 2005; Gomez-Gil *et al.*, 2011; Ranky and Adamovich, 2010; Shenoy *et al.*, 2008]].

Although this approach is similar to joint level control in requiring continuous attention to a relatively large number of simultaneously, the user's control is directly in the task space. Control that is directly in the task space allows the user to more easily decouple the different controlled degrees of freedom. This makes it more practical to use facial muscles for control for a number of reasons. First, because facial muscles are close together, it is more complicated to separate the source of the input signals picked up by an electrode at a particular muscle site if several muscles are activated at the same time. Additionally, control over these muscles is generally less fine grained, as individuals generally don't use their facial muscles for fine manipulation. Being able to decouple the controlled degrees of freedom can allow the user to make reasonable progress towards their goal while closely attending to only one degree of freedom at a time, which makes predictable, fine grained control less important.

2.1.5 Discrete Mode Control

In discrete mode control, the user is able to switch between a set of predetermined configurations. The aformentioned control methods involve control over some continuous state space. These modes require continuous user attention, high data rates, and require a great deal of understanding of the robot itself from the individual. Additionally, because manipulators are have a large number of degrees of freedom, these continuous methods do not attempt to control them at all. Rather, they switch the manipulator between two simple discrete states, open and closed. In some paradigms, the user is able to switch between a number of different discrete modes that control the configuration of the hand[*Yang et al.*, 2009; *Woczowski and Kurzyski*, 2010; *Ho et al.*, 2011; *Cipriani et al.*, 2008; *Matrone et al.*, 2011].

These control schemes represent a tradeoff between flexibility and simplicity of use. This tradeoff is especially important for complex, multijointed robotic hands. Direct control over the fingers of a manipulator is not feasible for more complex hands for a number of reasons. There are generally many degrees of freedom, and the configuration of each finger is important to whether the hand will unintentionally interact with the environment as the end effector is used. Additionally, the fingers may have overlapping workspaces, so without extremely accurate control, it is likely that they will hit each other. By allowing the user to switch between discrete states, they are able to get utility out of hands that are more complex than the simple grippers that are generally used in the simple open/close schemes. More complex hands can more accurately approximate the surface of the object that the user wants to interact with, which increases the number of possible interactions and makes them more stable.

However, these schemes limit the user's flexibility to the preset configurations. Additionally, the user has to remember how to get to the configuration that they want to use at a given time, which may require multiple steps through a branching decision tree. In continuous control schemes, the user can make small changes and observe the outcome to get the robot to do what they want, but in discrete control scheme the result of the next input may not be related to the previous one. Because there is not necessarily an easy way of associating the path that they need to take in that decision tree with the goal they want to reach, these control schemes have a high learning curve.

2.1.6 Task Level Control

The key challenge of using noninvasive brain computer interfaces is that the bit rate is low and that the input is somewhat unreliable. In addition, the user experiences limited feedback, which makes direct control difficult. Under these conditions, it would seem intuitive that users would find task level control, where the user directs the robot on what to do but has little input as to how, would be more effective. Indeed, it has been shown that users find BCI control easier using even higher level, goal oriented paradigms [Royer *et al.*, 2011], and we have begun to see work that attempts to exploit higher level abstractions to allow users to perform more complex tasks with robotic arms.

In [Bell *et al.*, 2008], EEG signals were used to select targets for pick and place operations for a small humanoid robot. [Waytowich *et al.*,] used EEG signals to control pick and place operations of a 4-DOF St aubli robot. [M. Bryan, V. Thomas, G. Nicoll, L. Chang and Rao, 2011] presented preliminary work extending this approach to a grasping pipeline on the PR2 robot. In that work, a 3D perception pipeline is used to find and identify target objects for grasping and EEG signals are used to choose between them. In [Müller-Putz *et al.*, 2005], grasping is decomposed to a 4 stage pipeline where EEG signals are used to control transitions between stages. And in [Scherer *et al.*, 2011], the authors demonstrate an interface to navigate in two dimensions and select goals in a complex virtual environment and propose a hierarchical control scheme for learning high level tasks dynamically.

2.2 Robust Grasping

In this work, we will present users with appropriate grasps for the object. The system will present the user with options, and they will select the option that best reflects their intent. Because the user does not exercise direct control over grasp acquisition, we need to be able to present the user with grasps that the manipulator can acquire reliably in the face of sensor noise. Analyzing the robustness of a grasp in the presence of object localization errors and external force perturbations is an important and difficult problem, which has thus been studied by a large number of researchers following many different strategies.

2.2.1 Wrench Space Metrics

A key criterion that has been used to define a stable grasp is that the contact points of the grasp are able to generate a wrench in an arbitrary direction, termed force closure. This property is considered fundamental in grasp analysis because it provides a simple, necessary condition for grasp stability, as shown by [Salisbury and Roth, 1983]. This property is determined by the set of wrenches that can be produced from the contact points of the grasp, termed the grasp wrench space (GWS). Force closure provides a binary analysis of grasp robustness. In order to analyze the strength of the force closure, we commonly use the epsilon quality (ϵ_{GWS}), first described in [Ferrari and Canny, 1992]. ϵ_{GWS} is defined as the radius of the largest ball around the origin that fits in the convex hull of the grasps contact wrench space. This radius is the magnitude of the minimum norm wrench that will break the object free of the grasp.

2.2.2 Wrench Space Metrics Robust to Contact Location Uncertainty

In previous work, measures have been proposed to quantify the robustness of contact location based quality metrics, with particular focus on the ϵ_{GWS} . One well developed approach considers the effect of contact model or contact location uncertainty with respect to the object. The independent contact region approach (ICR) introduced in [?] considers the effect of contact location uncertainty on the ϵ_{GWS} of a grasp. This approach grows a convex set of acceptable contact locations for each planned finger contact on the object. Any set of contact locations chosen from this set produces a grasp whose quality metric is lower bounded by a preselected quality threshold. Faverjon et. al. developed analytical approaches to finding ICRs for complex 2D and simple 3D models[Ponce and Faverjon, 1991; Ponce *et al.*, 1996; Faverjon and Ponce, 1991]. In Roa and Suarez [Roa and Suarez, 2009], this approach is extended to complex three dimensional shapes and minimal thresholds on the ϵ_{GWS} . [Pollard , 2004] followed a similar approach with a focus on larger numbers of original contacts and with extensions to task wrench space quality metrics, and also presented a method for generalizing sets of ICRs between objects. Zheng and Qian proposed a quality metric based on a similar region growing approach by measuring the radius of the smallest ball in the configuration space of the regions produced for the grasp parametrized

by contact location, contact normal, or frictional coefficients[Zheng and Qian, 2005]. All of these approaches consider the effects of contact location uncertainty independently, but do not directly address the effect of calibration error and object pose uncertainty on the ϵ_{GWS} . These approaches assume that uncertainty causes the contacts to land near the planned contact points on the object. However, simulating the entire grasping procedure often produces very different sets of contacts in the presence of uncertainty. In fact, none of the ICR approaches described are able to fully account for the effects of these resulting deviations from the planned contact locations.

2.2.3 Simplified Analytical models of Robustness

Rather than analyzing the wrench space of the applied grasp, another approach to grasp synthesis is to model the fingers as a point or hemisphere where the contacts are represented as a set of spring-like elements connect the finger to the object. With this simplification, it is possible to analytically calculate the wrench applied to the object by the fingers. By using some optimization approach, it is then possible to find the joint torques that apply zero total wrench to the object while maintaining some minimum internal force which stabilizes the object through friction. By combining this approach with assumptions about the geometry of the fingertip and the smoothness of the contact location on the object, it is possible to use an analytical approach or an optimization approach to find regions with large stability boundaries using the same joint torques. Such models have been pursued by authors under some simplified conditions in 2D [Sugar and Kumar, 2000] or simple 3D models with simple contact formulations[Yamada *et al.*, 2001]. However, it is not clear how to generalize these results to arbitrary hands and objects. Additionally, these models require many parameters of the analytical model to be chosen ad hoc.

This methodology shows promise, but hasn't been demonstrated outside of these highly simplified situations.

2.2.4 Sampling Based Heuristics

Some work has addressed the effect of object pose uncertainty in grasping tasks for measures of grasp stability other than the ϵ_{GWS} . In Balasubramanian et al. the authors derive

a novel grasp measure for robust grasping from observations of human guided grasping [Balasubramanian *et al.*, 2010]. Bekiroglu et al. proposed a method to learn haptic features of grasp stability to assess grasps during their execution[Bekiroglu *et al.*, 2011]. The general problem of motion and manipulation planning robust to pose error was addressed by by Lozano-Perez et. al [Lozano-Prez *et al.*, 1984] using preimage-backchaining. In [Berenson *et al.*, 2009], this method was extended to hand target pose regions for grasping objects on a table top. In [Brost and Christiansen, 1997], Brost and Christiansen investigated the issue of pose error robustness for a 2D gripper using a sampling based approach on a fixed trajectory plan in physical experiments. More recently, [Hsiao *et al.*, 2011] investigated Bayesian approaches to grasp planning under object pose and identity uncertainty for a simple gripper using a sampling approach to select robust grasps as measured by a grasp quality metric in simulation .

This approach is the most generic, simplest to understand, and the easiest to implement. We have followed a similar approach in analyzing the grasps produced by our grasp planner.

Chapter 3

Robust Grasping

3.1 Grasp Planning with Contact Points

Analytical models analyzing the probability of grasp success have not been found, and so far the most generic methods involve sampling. The configuration space of the “grasping” problem has several formulations, but the two most common are potential contact points or hand configurations. In analyzing potential contact points, one can either analyze points on the hand or on the object. There are numerous considerations that one can take into account that make intuitive heuristic sense, including geometric concerns such as local flatness.

Historically, it has been common to analyze the forces that can be applied at each contact point. There are no perfect models for this analysis. Models are generally classified by the physical systems that they roughly approximate. A point contact model assumes that the contact point can only apply forces in the direction opposite the normal of the surface on which it contacts. This is a conservative model. In order to generate a stable grasp from point contacts, it is necessary that any small (i.e. differential) motion cause the object to overlap the proposed contact points. This is called *form closure*. This is the equivalent of the positive span of the contact normals covering the entire space. This is an example of *form closure*. For point contacts, these constraints are *duals*, and one strictly implies the other. For the rest of the contact models which take friction into account, this is not the case - one can have *force close* without *form closure*.

This model is simple and conservative, but unfortunately it is too conservative to be use-

ful for arbitrary objects. If rotations are considered, cylindrical objects cannot be through *form closure*, because there is no contact normal that can oppose rotations along the length of the cylinder. More generic models include frictional forces in addition to pure normal forces. Point contact with friction models allow friction to be employed at each of the contact points in the plane orthogonal to the normal. In this case, the forces that can be produced at the contact point through friction are related to the normal force through the friction coefficient of the surface. This creates a cone of potential forces that can be created as the normal forces are scaled up.

Further, if the contacting surface is assumed to be ‘soft’ so that one surface conforms to another forming a contact patch, rather than a point, the contact can also apply torque around the normal direction. If the surface is significantly softer, the patch can be modelled as a set of points on the perimeter of the patch. These points will be able to apply torques around all three dimensions with respect to the original contact point, and forces along any direction in the positive halfspace of the surface normal.

In order to analyze how the contact forces effect the object, the forces and torques need to be summed up in the same reference frame. Most often, they are transformed to the centroid of the surface mesh or to the center of mass, if known. Transforming the cone of forces that can be produced by the point with friction model, because it is cannot be represented by a linear model, and so the linear transform to the new reference frame leads to a complex representation. In order to avoid this, the cone is represented by a simple linearization, making the base of the shape a regular polygon rather than a circle. Then the potential forces can be represented by the edges from the contact point to the points on the perimeter, normalized by the number of edges.

3.2 Grasp Wrench Spaces

To characterize the contribution of the contact wrenches to constructing stable grasps, we need a way to analyze the whole set of wrenches wholistically. Irrespective of the contact model used, so long as it is linearized, the contacts can be summed up in the same reference frame, and all potential forces that could possibly be generated by these contact points can

be represented. This set of forces is called the “Grasp Wrench Space.” In plain terms, the Grasp Wrench Space represents the set of wrenches that can be applied by this grasp. A key criterion that is often used to define a successful grasp is the ability to generate a wrench in an arbitrary direction, which is the generic definition of *force closure*. This property is considered fundamental in grasp analysis because it provides a simple, necessary condition for grasp stability[Salisbury and Roth, 1983].

3.3 The ϵ_{GWS} Quality Metric

The ϵ_{GWS} metric of grasping extends force closure from a binary property which is or is not satisfied to a measure of how stable a grasp is with respect to grasp forces. The ϵ_{GWS} measure is one of the most widely cited benchmark metrics in the grasp planning field[Ferrari and Canny, 1992]. Formally, for a set of contact wrenches $C \subset R^6$, one can define the neighborhood ball $B(\epsilon)$ and wrench space metric ϵ_{GWS} as follows:

$$B(\epsilon) = \{x \in R^6 \mid \|x\|_2 < \epsilon\}$$

$$\epsilon_{GWS}(C) = \max_{\epsilon} [B(\epsilon) \subseteq \text{convexhull}(C)]$$

Any grasp that does meet the minimum requirement of an $\epsilon_{GWS} > 0$ cannot apply force in some direction, which means that some infinitely small force in that direction will cause the object to begin to move. This quality metric is popular largely because it analytically addresses an intuitively necessary condition for grasp stability, the ability to resist force perturbations. One shortcoming of this measure is that it is sensitive to the choice of center of mass of the object. A variant of this measure is to consider the volume of $\text{convexhull}(C)$, denoted V_{GWS} in this work. This variant functions as an approximation of the average case ϵ_{GWS} over many estimations of the center of mass of the object.

3.4 Optimization Based Grasp Planning

Given a quality measure that is computationally tractable, it is feasible to create a stochastic optimization based grasp planner. Sampling potential contact points directly on the object leaves the problem of finding a hand configuration that matches that contact configuration

unsolved. For the generic case of arbitrary hands, this problem is difficult and unsolved. Similarly, sampling candidate contact points on the hand is equally intractable, because most hand configurations produce no contacts at all. To make the problem tractable, the state space needs to be relatively low dimensional and the quality metric must generate valid, informative values on most of that state space.

3.4.1 Potential Contact Quality Function

This lab has produced a planner that uses such a measure with simulated annealing based optimization. To make the quality metric accessible to this method and more computationally tractable, the potential contact points on the hand are projected to the object and the resulting contact wrenches are weighted by their distance and the agreement of their normal directions. This “potential contact” quality function creates a smoother optimization function.

3.4.2 Implications for pose error robustness

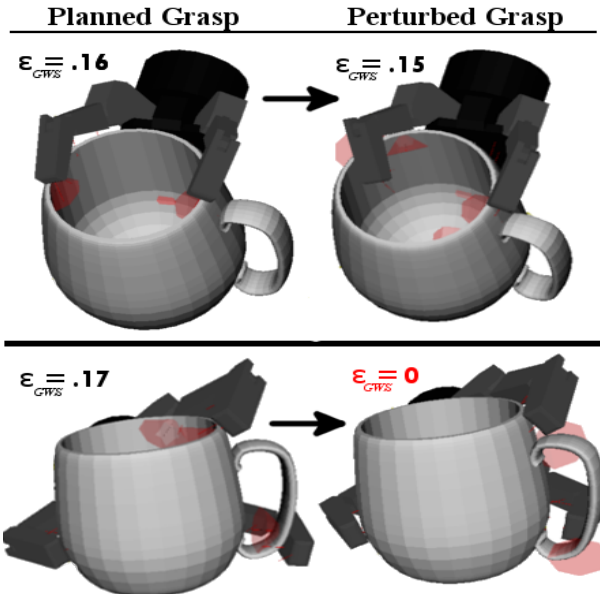


Figure 3.1: An example of a grasp where the ϵ_{GWS} is consistent with respect to the common localization errors, and one where it is not.

A stochastic optimization based approach is capable of escaping local minima in complex, nonconvex optimization functions like the projected distance and alignment between nonconvex shapes. However, the net effect of the optimization procedure is still to approximately follow a gradient. We should thus expect that the most optimal grasps that are found should usually be found in areas where the quality function is fairly smooth and the basin of attraction is wide. Given the quality function, especially the component which takes into account the relative alignment of the potential contact location and the hand, it follows that the local geometry should be expected to be relatively smooth, and that the quality function, when evaluated, should be robust to small errors in contact location.

However, in real robotic applications, if the object is known then the largest sources of contact location uncertainty are errors in perception of the location of the object itself with respect to the robot, miscalibration of the robot, and intrinsic uncertainty in control of the end effector's location. This implies that the errors in contact location are not randomly distributed, but are structured, in that they are offset in the same direction because the entire object is offset. In fact, the actual contact location is a product of the entire grasping procedure, in which a different part of the finger may make contact than is planned, and this contact location not be near the planned location. The normals may face a different enough orientation that the smoothness of the projected contact point's quality function may not be sufficient to guarantee that the actually achieved contact points produce a stable grasp. Some planned grasps may have nearly the same quality measure if the object's pose is slightly perturbed, while others may not. Fig. 3.1 shows an example of each.

3.5 Analyzing The Effects of Pose Error In Simulation

3.5.1 The Columbia Grasp Database

In order to test how robust the grasps that are produced by this planner are to localization errors, we need a large database of grasps. The Columbia Grasp Database (CGDB) had already been produced by [?] to seed a machine learning based approach to grasp planning. The CGDB was constructed by using the Eigengrasp planner on the Princeton Shape Benchmark, a set of 1814 models with class labels. Starting from this set of grasps,

we developed a simulation model to estimate the effects of localization error across many objects.

3.5.2 Grasping Pipeline

The CGDB parametrizes grasps as pre-grasp and final-grasp pairs. The pre-grasp is a collision free pose and joint angle set found by the simulated annealing planner. The final-grasp is the set of corresponding parameters found by applying a grasping heuristic to the pre-grasp that simulates closing the hand around the object until contact is made or joint limits are reached. The grasps in the CGDB are intended to be used by preshaping the hand to the pre-grasp under the assumption this is a collision free pose, but in the presence of uncertainty this may not be the case for all grasps. In this case, it is necessary to generate an initial pose which is certain to be collision free.

The general problem of optimal hand trajectory planning for grasping is complex. In this work we consider a basic three-phase grasping heuristic.

- 1a.** Move hand and fingers to an initial pose and posture far from the object along a pre-specified approach direction.
- 1b.** Move to the planned pre-grasp hand pose from the initial pose along the approach direction, stopping if contact is made.
- 2a.** Move fingers to their pre-grasp postures by linearly interpolating from initial posture, stopping each finger if contact is made.
- 2b.** (optional) For grasps with any contact points that are not on a distal most link of a finger, approach object to contact if none has occurred so far.
- 3.** Close fingers until each joint is constrained by contact or joint limits.

We use the normal to the center of the palm as the approach directions for all of the grasps considered. To determine the finger positions for the initial posture, we open the fingers so that the hand in the initial pose can wrap around itself in the pre-grasp position. We illustrate this strategy in Fig. 3.2. We open the hand at a constant rate for all joints until

the tips of each finger are outside of the projection of the second most distal link along the approach direction of the hand in the planned pre-grasp pose.

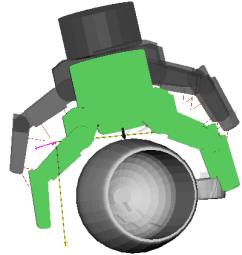


Figure 3.2: *Illustration of the initial pose and posture.* The hand is withdrawn along its approach direction and all of the fingers opened at the same constant velocity until each of the fingertips are outside of the knuckles of the hand in its pre-grasp configuration. The hand is then opened an additional ten percent of the remaining joint range. The pre-grasp configuration is shown in green.

3.5.3 Model of Pose Uncertainty

Because it is computationally intractable to densely sample the full six dimensional space of poses near the planned pregrasp pose, we consider a three dimensional error model representing an object on a support surface. We assume that each object is restricted to a set of stable poses on the surface. This error model is parametrized by $[x, y, \theta]$ as illustrated by Fig. 3.3. We use the centroid of the planned contact locations as the origin of the object because parameterizing the rotation around the center of mass of the object will have a disproportionate effect on grasps planned further from the center of mass. A reasonable range to explore using this parametrization should allow each parameter to move the relative position of the planned grasp's contact point by at least 10 mm. If we make the rough approximation that the projection of the contact points perpendicular to the axis of rotation lie on a circle with a 5 cm radius, a reasonable range for these parameters is $\theta \in [-20^\circ, 20^\circ]$ and $x, y \in [-10\text{mm}, 10\text{mm}]$. These bounds are motivated by our anecdotal experience in aligning a known object to a point cloud using common methodologies. Exploring this parameter space uniformly in increments of $1[\text{mm}, {}^\circ]$ in simulation requires 18,081 simulations

per grasp. Using the GraspIt! grasping simulator[?] on a Xeon 2.67GHZ processor we can perform this many kinematic simulations of the grasping pipeline in under two hours for the worst case. The time required for each simulation is object and grasp dependent. With cluster computing this approach can be used to analyze large numbers of grasps from a database off-line.

3.5.4 Simulation Results

These simulations resulted in a large dataset of grasps, perturbations from planned positions, and associated quality functions. From this data, we sought to answer two questions. First, how well do the quality measures of the planned grasp predict expected grasp qualities after perturbation. Second, how do grasp qualities effect the probability of attaining a *force-closed* grasp in the presence of pose uncertainty.

3.5.4.1 Expected Grasp Quality

The grasps we analyzed were produced by the optimization procedure described in section . As we argued previously, it is reasonable to expect that the grasps produced by that planner should be locally near optimal with respect the hand position. The resulting planned grasps

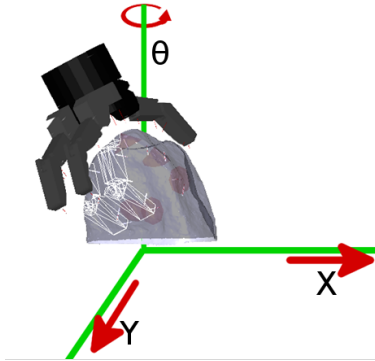


Figure 3.3: Illustration of the tabletop error model used in this paper. The object is can be translated $[-10, 10]$ mm in both X and Y and rotated $[-20, 20]^\circ$ around θ . The red cones mark the planned contact points. The white wire frame indicates the planned end configuration of the fingers.

are thus locally optimal with respect to the pose of the hand. To quantify how much the imposed pose perturbation effects a particular grasp, we can look at the expected value and standard deviation of its ϵ_{GWS} and V_{GWS} . However, to understand these effects on average across many grasps and objects, we normalize the expected value and standard deviation of these qualities by the quality values of the planned grasp with no error. We call the simulated quality measures of the planned grasp with no error the 'planned' quality values. Because the planned quality values are locally optimal, the expected value of the quality normalized to the planned value should have a maximum value of 1 for very robust grasps and a minimum value of 0 for extremely fragile grasps. We then consider the average of these quantities across all 480 grasps.

3.5.4.2 Probability of Achieving Force Closure

Another important measure that contributes to grasp success is how likely the perturbed grasp is to fail to be *force-closed*(*fc*), which is defined as having an $\epsilon_{GWS} = 0$. These grasps are expected to be fundamentally unstable, and so a grasp with a higher average quality but a larger variance, leading to more non-*fc* positions may succeed less often than a grasp with a lower average quality that has lower variance. To measure this effect directly, we counted the number of *fc* grasps of the perturbed samples and divided that by the total number of samples, giving us a measure we have called $P(fc)$, as it represents the probability of achieving a force closed grasp given that our sampled perturbations are uniformly likely.

Calculations involving convex hulls, such as the ϵ_{GWS} are known to be sensitive to numerical inaccuracies, and the cluster we used to generate this dataset was heterogeneous in both hardware and software environments. This initially lead to grasps that appeared *fc* with a small ϵ_{GWS} values to appear non-*fc* when evaluated on a different machine in the cluster. To achieve consistent results, we had to chose an arbitrary small positive δ that is larger than the cross-machine variability that we observed, and redefine *fc* to require that $\epsilon_{GWS} > \delta$. In this work, we arbitrarily chose $\delta > 0.001$, as this was several orders of magnitude above the largest discrepancy we ever observed between two machines analyzing the same grasp, and several orders of magnitude lower than the quality of the average unperturbed grasp that we evaluated.

Measure across sampled perturbations	Average across 'Tool' grasp dataset
normalized expected ϵ_{GWS}	0.5091
normalized std(ϵ_{GWS})	0.2915
normalized expected V_{GWS}	0.679
normalized std(V_{GWS})	0.3588
$P(fc)$	0.7957

Table 3.1: Summary of Simulation Results: These results quantify how robust each quality measure is to pose uncertainty. For each grasp, the expected value and standard deviation of the respective quality measures are calculated across the poses sampled. These measures are normalized by dividing them by the planned quality of the unperturbed grasp to allow comparison of the effects of uncertainty across grasps. $P(fc)$ denotes the measured probability of achieving a force closed grasp, which we have calculated as $P(\epsilon_{GWS} > .001)$

We calculated these statistics across all of our grasps. These results are summarized in Table 3.2. We see that the expected ϵ_{GWS} and V_{GWS} are 50% and 67% of their planned values, respectively. This shows that pose uncertainty has a large effect on the expected value of these measures. Additionally, we see that there relatively high variance of these measures across all of the sampled perturbations for a single grasp. The average standard deviation of the measures across the perturbed samples of a single grasp is 29% of the ϵ_{GWS} and 35% of the V_{GWS} .

The observation that the within grasp variability is high is what led us to consider whether the number of non- fc perturbed samples varied significantly across grasps with similar ϵ_{GWS} qualities. We found that the average $P(fc)$ is around 80%. This implies that even the best five grasps for the object should be expected to fail 20% of the time, if we only filter grasps by their ϵ_{GWS} quality.

3.5.5 Chosing optimal grasps: ϵ_{GWS} vs $P(fc)$

In the case of chosing a single grasp out of a set of many, we are faced with the problem of ranking grasps. The fundamental question we seek to answer with these research can be

rephased simply as whether performing that ranking relying solely on the ϵ_{GWS} is sufficient to chose the grasp most likely to achieve stable *force – closure* in the presence of location uncertainty. .

In Fig.3.4, we have plotted the planned ϵ_{GWS} against the estimate of the probability of achieving force closure, for each grasp. $\overline{\epsilon}^*_{GWS}$ indicates the average ϵ_{GWS} for the best grasp available for each object, which is 0.095. For most objects, the best grasp by ϵ_{GWS} lies in the range where $\epsilon_{GWS} \in (0, 0.2)$, bordered by the red line on the right of the figure. This figure shows that there is no correlation between ϵ_{GWS} and $P(fc)$ in that range.

This implies that the ϵ_{GWS} cannot be used to chose grasps that are expected to be robust. On average the best grasp by $P(fc)$ for each object has a $P(fc)$ which is .21 greater than the $P(fc)$ of the highest ϵ_{GWS} grasp. Under the error model described, choosing the highest $P(fc)$ grasp will result in a force closed grasp 21% percent more often than choosing the best grasp by ϵ_{GWS} . This analysis yields approximately the same results for the V_{GWS} in comparison to the $P(fc)$.

3.6 Physical Experiments

These simulation results show that using $P(fc)$ as a quality metric for ranking grasps from a database may select grasps which are more reliable in the face of object pose estimation error. To test whether these simulation results can be verified against physical experiments, we attempted to grasp ten objects for which we had high quality mesh models readily available courtesy of the the DARPA ARM-S project and the Willow Garage object database [23]. We added these models to our database, and calculated the $P(fc)$ for the top five grasps by ϵ_{GWS} value.

To test these grasps on a real robotic grasping system we used a Barrett 280 model hand attached to a Staubli TX60L 6 degree of freedom arm to implement the grasping pipeline described in section II-A. To emulate the friction coefficient used in our simulations, we wrapped the contacting surfaces of the hand in rubberized shelf liner. One object attempted was a blue detergent bottle made of very smooth plastic. We added a rubberized tape to the contact locations on this object to increase its friction coefficient. For each object, we

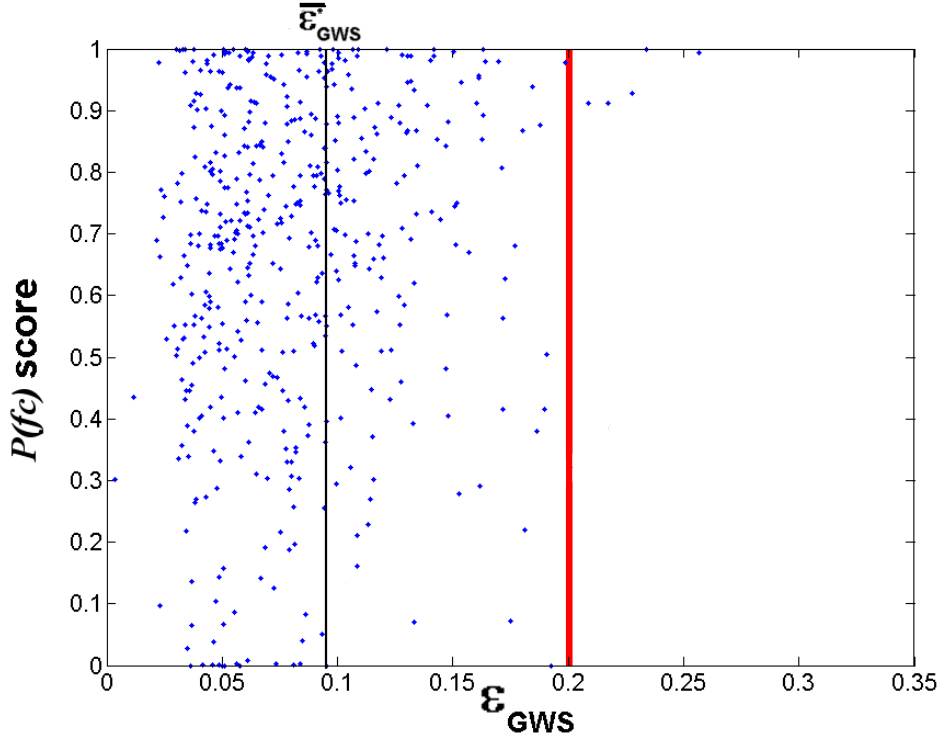


Figure 3.4: ϵ_{GWS} plotted against $P(fc)$, which is equivalent to the probability of attaining a force closed grasp under our error model from a planned starting grasp configuration. 480 grasps over 96 objects are presented in this figure. This figure demonstrates that the ϵ_{GWS} is generally a poor predictor of pose error robustness as measured by the $P(fc)$. The mean ϵ_{GWS} , denoted by the black line, is 0.095. There appears to be a cutoff, denoted by a red vertical line on the graph, around $\epsilon_{GWS} > 0.2$, after which all available grasps have a high $P(fc)$, but note how few grasps there are in the database with quality values that high. Only five objects have a grasp with a quality that high, which implies that for most objects, ϵ_{GWS} cannot be used to predict $P(fc)$.

selected the best grasp ranked by ϵ_{GWS} and the best grasp ranked by $P(fc)$. The objects were calibrated to the robot using a printed template of the bottom outline of the objects. We align the edge of each template to a known coordinate system in our robots workspace. We selected a perturbed position by sampling our error model and then applying the grasp pipeline as though the objects origin was at the perturbed location.

We tested up to ten randomly selected perturbed positions for each grasp. The same perturbations were applied to both of the tested grasps for each object. We moved the arm and hand at very slow speeds to simulate quasi-static conditions. In the first two stages of the pipeline, we moved the arm at 1% of its maximum speed, and the fingers of the Barrett hand at 10% of their maximum speed. In the final closing step, initial contact had been achieved or joint limits have been reached for each finger. We then raised the finger speed to 50% to drive the underactuated fingers to their final positions. After the fingers stopped moving, we lifted the object 3 cm perpendicular to the tables surface. If any part of the object was still touching the table when the arm came to a stop, we graded the trial as a failure, otherwise we graded the trial as a success.

We find that the grasps ranked best by the $P(fc)$ are successful more often. The results of this experiment along with the grasps and objects analyzed are in Fig. 3.5 and Fig. 3.6. Overall, for these ten objects the $P(fc)$ ranking selected successful grasps on 85 out of 93 trials (91%), whereas the grasps selected by the ϵ_{GWS} ranking succeeded on 63 of 93 trials (67%). For some objects, nearly all of the grasp attempts were successful irrespective of the $P(fc)$ score. We separated the objects in our experiment into two groups. One group is composed of larger, more complex objects shown in Fig. 3.6 and the other group is composed of light, roughly cylindrical objects shown in Fig. 3.5. We see that all of the objects in the roughly cylindrical category were grasped very robustly irrespective of $P(fc)$ score. For these objects, the Eigengrasp planner finds grasps which more or less encompass the object. In contrast, for the five objects which could not be enveloped by the hand, we see that the $P(fc)$ ranked grasp is successful in 35 out of 43 trials (81%), as compared to 16 out of 43 trials (37%) using the ϵ_{GWS} grasp. These results show that the $P(fc)$ ranking chooses more successful grasps; especially on the larger, more complex objects where the success rate is doubled.

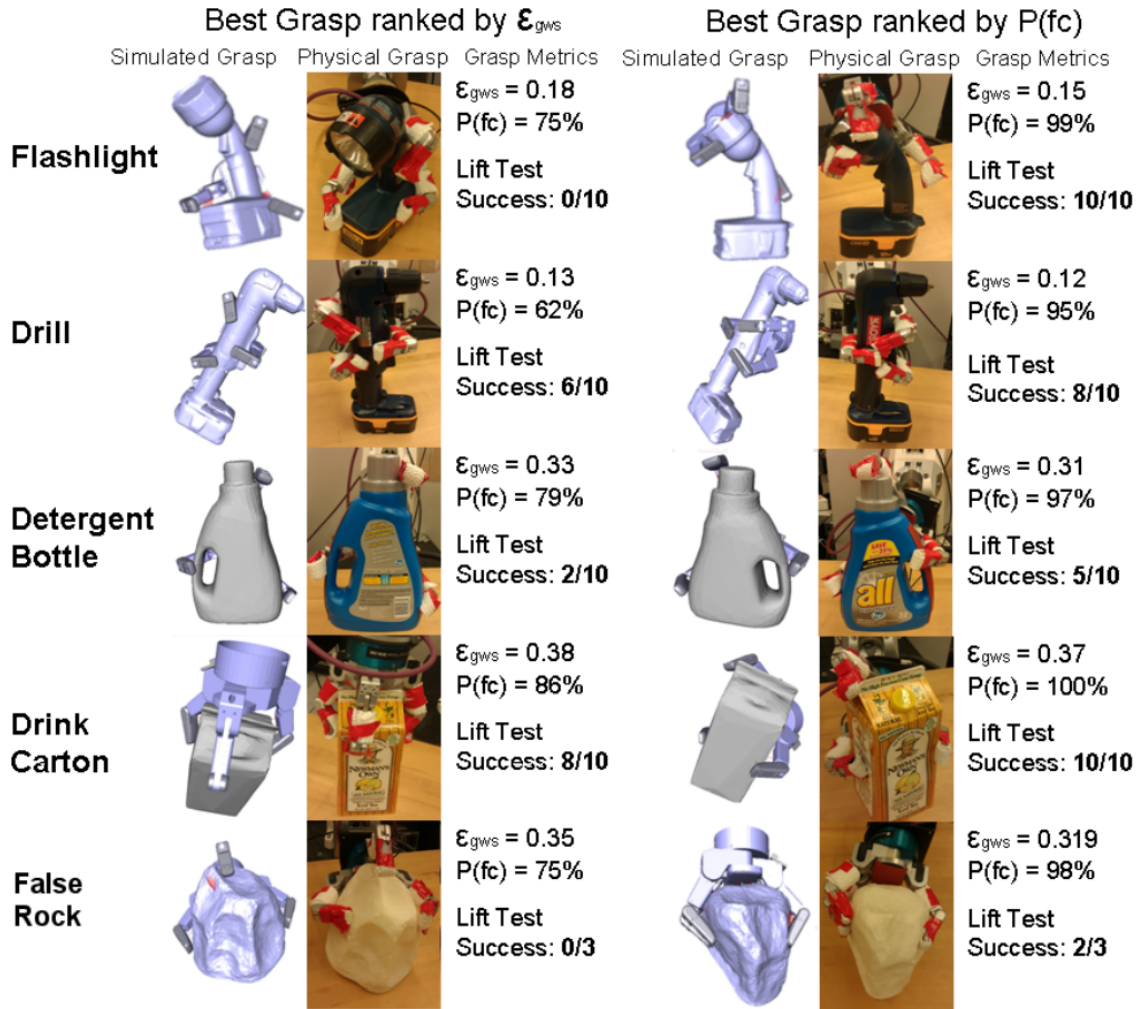


Figure 3.5: *Results A*: The results of physical experiments on five large, complex objects. In the left column are the best grasps for each object ranked by ϵ_{GWS} . An example of the simulated and physically realized grasp is illustrated for each grasp attempted. Additionally, the figure gives the $P(fc)$ and ϵ_{GWS} for each grasp attempted, as well as the fraction of attempts which succeeded in lifting the object by 3 cm in physical experiments. The higher $P(fc)$ grasp is successful on many more trials than the higher ϵ_{GWS} grasp for these objects.



Figure 3.6: *Results B*: The results of physical experiments on five smaller, simpler objects. In the left column are the best grasps for each object ranked by ϵ_{GWS} . In the right column are the best grasps by $P(fc)$. An example of the simulated and physically realized grasp is illustrated for each grasp attempted. Additionally, the figure gives the $P(fc)$ and ϵ_{GWS} for each grasp attempted, as well as the fraction of attempts which succeeded in lifting the object by 3 cm in physical experiments.

3.7 Discussion

In this work, we have shown that the planned ϵ_{GWS} of a planned grasp is not predictive of the probability of achieving a force closed grasp in the presence of uncertainty, neither in simulation nor physical experiments. To analyze this in simulation we generated the measure $P(fc)$ as an approximation of this probability. We then showed that the $P(fc)$ can itself be used to rank grasps from a preplanned grasp database and that this reranking predicts grasping success in physical experiments better than the ϵ_{GWS} .

The analysis presented here is less effective at discriminating fragile grasps on smaller objects than it is on larger objects. For small objects, the object is fully encompassed by the hand, and the highest ϵ_{GWS} grasp is always an enveloping powergrasp, and are always spherical, as described in [?]. As seen in 3.6, in such grasps the palm behind is behind the object, one finger pressing downwards, with each finger roughly evenly spaced apart. For a hand capable of achieving this configuration, it is always a high ϵ_{GWS} grasp, because the normals of the contact points are evenly spaced around the center of the grasp, which maximizes their ability to directly oppose perturbation forces. It is also a configuration which is relatively invariant to perturbations that do not move the object outside of the working envelope of the hand.

Under more constrained conditions, such grasps are not always attainable. The object may not be in the center of the workspace, there may be objects in the way, or the desired purpose to which the object will be put requires a different grasp. These cases are better represented by the results on the large objects, which couldn't be fully encompassed by the hand. Under these conditions, the higher ϵ_{GWS} grasp often fails, and we see better results ranking by $P(fc)$

3.7.1 Online Extensions

Although the full sampling rate is too computationally expensive, in Table 3 we examine the possibility of approximating $P(fc)$ at lower sampling rates. By using a sampling step size of (10mm, 10mm, 10 °), we see an average difference of 6% with respect to the denser sampling. In none of our samples did this change the order of our rankings. At this sampling

Sampling Step Size (X, Y, θ) (mm, mm, $^{\circ}$)	Mean Difference	Standard Deviation	Max Difference
2-2-4	0.0128	0.0122	0.0667
2-2-4(random)	0.0097	0.0086	0.0493
10-10-10	0.0653	0.0551	0.3205
10-10-20	0.0840	0.0713	0.4782

Table 3.2: This table quantifies the effect of sampling parameters on the estimate of quality measure. The first column describes the sampling density along each dimension of the error model. The other columns describe the average change in the subsampled $P(fc)$ as compared to the densest sampling rate. This demonstrates that

rate, we can generate an estimate in under a second, which make it suitable as a filter for an online grasp planning system. At lower sampling rates, the rankings do become reordered, which may lead us to select less robust grasps. In our shared control online planner, we use the lower resolution $P(fc)$ to weight the grasp quality measure that controls the order in which grasps are tested for reachability, and the order in which they are presented to the user. Without this filter, many grasps that are presented to the user are fragile to object pose estimation errors.

Part I

Bibliography

Bibliography

- [Artemiadis and Kyriakopoulos, 2011] Panagiotis K Artemiadis and Kostas J Kyriakopoulos. A switching regime model for the EMG-based control of a robot arm. *IEEE Trans. on Systems, Man, and Cybernetics*, 41(1):53–63, February 2011.
- [Balasubramanian *et al.*, 2010] R. Balasubramanian, Ling Xu, P.D. Brook, J.R. Smith, and Y. Matsuoka. Human-guided grasp measures improve grasp robustness on physical robot. In *Robotics and Automation (ICRA), 2010 IEEE International Conference on*, pages 2294–2301, May 2010.
- [Bekiroglu *et al.*, 2011] Yasemin Bekiroglu, J. Laaksonen, Jimmy Alison Jorgensen, V. Kyrki, and D. Kragic. Assessing grasp stability based on learning and haptic data. *Robotics, IEEE Transactions on*, 27(3):616–629, June 2011.
- [Bell *et al.*, 2008] Christian J Bell, Pradeep Shenoy, Rawichote Chalodhorn, and Rajesh P N Rao. Control of a humanoid robot by a noninvasive brain-computer interface in humans. *Journal of Neural Engineering*, 5(2):214–20, Jun 2008.
- [Berenson *et al.*, 2009] Dmitry Berenson, Siddhartha S. Srinivasa, and James J. Kuffner. Addressing pose uncertainty in manipulation planning using task space regions. In *in Proc. IEEE/RSJ International Conference on Intelligent Robots and Systems (IROS*, 2009.
- [Brost and Christiansen, 1997] RandyC. Brost and AlanD. Christiansen. Empirical verification of fine-motion planning theories. In Oussama Khatib and J.Kenneth Salisbury, editors, *Experimental Robotics IV*, volume 223 of *Lecture Notes in Control and Information Sciences*, pages 475–485. Springer Berlin Heidelberg, 1997.

- [Castellini and van der Smagt, 2009] Claudio Castellini and Patrick van der Smagt. Surface EMG in advanced hand prosthetics. *Biological cybernetics*, 100(1):35–47, January 2009.
- [Cipriani *et al.*, 2008] C. Cipriani, F. Zaccone, S. Micera, and M.C. Carrozza. On the Shared Control of an EMG-Controlled Prosthetic Hand: Analysis of User Prosthesis Interaction. *IEEE Transactions on Robotics*, 24(1):170–184, February 2008.
- [Faverjon and Ponce, 1991] B. Faverjon and J. Ponce. On computing two-finger force-closure grasps of curved 2d objects. In *Robotics and Automation, 1991. Proceedings., 1991 IEEE International Conference on*, pages 424–429 vol.1, Apr 1991.
- [Ferrari and Canny, 1992] C. Ferrari and J. Canny. Planning optimal grasps. In *Proc. of the Int. Conf. on Robotics and Automation*, pages 2290–2295, August 1992.
- [Gomez-Gil *et al.*, 2011] Jaime Gomez-Gil, Israel San-Jose-Gonzalez, Luis Fernando Nicolas-Alonso, and Sergio Alonso-Garcia. Steering a Tractor by Means of an EMG-Based Human-Machine Interface. *Sensors*, 11(7), 2011.
- [Grosz and Sidner, 1986] Barbara Grossz and Candace Sidner. Attention, intention, and the structure of discourse. *Computational Linguistics*, 12(3):175–204, July-September 1986.
- [Ho *et al.*, 2011] N. S. K. Ho, K. Y. Tong, X. L. Hu, K. L. Fung, X. J. Wei, W. Rong, and E. A. Susanto. An EMG-driven exoskeleton hand robotic training device on chronic stroke subjects: Task training system for stroke rehabilitation. In *Int. Conf. on Rehabilitation Robotics*, pages 1–5. IEEE, June 2011.
- [Horki *et al.*, 2011] Petar Horki, Teodoro Solis-Escalante, Christa Neuper, and Gernot Müller-Putz. Combined motor imagery and SSVEP based BCI control of a 2 DoF artificial upper limb. *Medical & Biological Engineering & Computing*, 49(5):567–77, May 2011.
- [Hsiao *et al.*, 2011] Kaijen Hsiao, Matei Ciocarlie, and Peter Brook. Bayesian grasp planning. 2011.

- [Lozano-Prez *et al.*, 1984] Toms Lozano-Prez, Matthew T. Mason, and Russell H. Taylor. Automatic synthesis of fine-motion strategies for robots. *The International Journal of Robotics Research*, 3(1):3–24, 1984.
- [M. Bryan, V. Thomas, G. Nicoll, L. Chang and Rao, 2011] J.R. Smith M. Bryan, V. Thomas, G. Nicoll, L. Chang and R.P.N. Rao. What You Think is What You Get: Brain-Controlled Interfacing for the PR2. Technical report, Iros 2011: The PR2 Workshop, San Francisco, 2011.
- [Matrone *et al.*, 2011] G. Matrone, C. Cipriani, M. C. Carrozza, and G. Magenes. Two-channel real-time EMG control of a dexterous hand prosthesis. In *Proc. Int. Conf. on Neural Engineering*, pages 554–557, April 2011.
- [Müller-Putz *et al.*, 2005] Gernot R Müller-Putz, Reinhold Scherer, Gert Pfurtscheller, and Rüdiger Rupp. EEG-based neuroprosthesis control: a step towards clinical practice. *Neuroscience Letters*, 382(1-2):169–74, 2005.
- [Pollard , 2004] Nancy Pollard . Closure and quality equivalence for efficient synthesis of grasps from examples. *International Journal of Robotics Research*, 23(6):595–614, 2004.
- [Ponce and Faverjon, 1991] J. Ponce and B. Faverjon. On computing three-finger force-closure grasps of polygonal objects. In *Advanced Robotics, 1991. 'Robots in Unstructured Environments', 91 ICAR., Fifth International Conference on*, pages 1018–1023 vol.2, June 1991.
- [Ponce *et al.*, 1996] Jean Ponce, Steve Sullivan, Attawith Sudsang, Jean daniel Boissonnat, and Jean-Pierre Merlet. On computing four-finger equilibrium and force-closure grasps of polyhedral objects. *International Journal of Robotics Research*, 16:11–35, 1996.
- [Postelnicu *et al.*, 2011] Cristian-cezar Postelnicu, Doru Talaba, and Madalina-ioana Toma. Controlling a Robotic Arm by Brainwaves and Eye. *Int. Fed. For Information Processing*, pages 157–164, 2011.

- [Ranky and Adamovich, 2010] G. N. Ranky and S. Adamovich. Analysis of a commercial EEG device for the control of a robot arm. In *Proc. Northeast Bioengineering Conference (NEBEC)*, pages 1–2, New York, NY, March 2010.
- [Roa and Suarez, 2009] M.A. Roa and R. Suarez. Computation of independent contact regions for grasping 3-d objects. *Robotics, IEEE Transactions on*, 25(4):839–850, Aug 2009.
- [Royer *et al.*, 2011] Audrey S Royer, Minn L Rose, and Bin He. Goal selection versus process control while learning to use a brain-computer interface. *Journal of Neural Engineering*, 8(3):036012, June 2011.
- [Sagawa and Kimura, 2005] K. Sagawa and O. Kimura. Control of robot manipulator using EMG generated from face. In *Proc. Int. Conf. on Manufacturing and Industrial Technologies*, volume 6042, December 2005.
- [Salisbury and Roth, 1983] J.K. Salisbury and B. Roth. Kinematic and force analysis of articulated mechanical hands. *Journal of Mechanical Design*, 105, March 1983.
- [Scherer *et al.*, 2011] Reinhold Scherer, Elisabeth C. V. Friedrich, Brendan Allison, Markus Pröll, Mike Chung, Willy Cheung, Rajesh P. N. Rao, Christa Neuper, and Markus Pr. Non-invasive brain-computer interfaces: enhanced gaming and robotic control. In *Advances in Computational Intelligence*, volume 6691. June 2011.
- [Schmidl, 1965] HANNES Schmidl. The inail myoelectric b/e prosthesis. *Orthop Prosthet Appl J*, pages 298–303, 1965.
- [Shenoy *et al.*, 2008] Pradeep Shenoy, Kai J Miller, Beau Crawford, and Rajesh N Rao. Online electromyographic control of a robotic prosthesis. *IEEE Transactions on Biomedical Engineering*, 55(3):1128–35, March 2008.
- [Sherman and Lippay, 1965] E David Sherman and Andrew Lippay. A russian bioelectric-controlled prosthesis. *Canadian Medical Association journal*, 92(5):243, 1965.

- [Sugar and Kumar, 2000] T.G. Sugar and V. Kumar. Metrics for analysis and optimization of grasps and fixtures. In *Robotics and Automation, 2000. Proceedings. ICRA '00. IEEE International Conference on*, volume 4, pages 3561–3566 vol.4, 2000.
- [Vogel *et al.*, 2010] Jörn Vogel, Sami Haddadin, John D Simeral, Sergej D Stavisky, Dirk Bacher, Leigh R Hochberg, John P Donoghue, and Patrick Van Der Smagt. Continuous Control of the DLR Light-weight Robot III by a human with tetraplegia using the Brain-Gate2 Neural Interface System. In *International Symposium on Experimental Robotics*, 2010.
- [Waytowich *et al.*,] N. Waytowich, A. Henderson, D. Krusienski, and D. Cox. Robot application of a brain computer interface to staubli TX40 robots - early stages. *World Automation Congress (WAC)*, pages 1–6.
- [Woczowski and Kurzyski, 2010] Andrzej Woczowski and Marek Kurzyski. Human-machine interface in bioprostheses control using EMG signal classification. *Expert Systems*, 27(1):53–70, February 2010.
- [Yamada *et al.*, 2001] T. Yamada, T. Koishikura, Y. Mizuno, N. Mimura, and Y. Funahashi. Stability analysis of 3d grasps by a multifingered hand. In *Robotics and Automation, 2001. Proceedings 2001 ICRA. IEEE International Conference on*, volume 3, pages 2466–2473 vol.3, 2001.
- [Yang *et al.*, 2009] Dapeng Yang, Jingdong Zhao, Yikun Gu, Li Jiang, and Hong Liu. EMG pattern recognition and grasping force estimation: Improvement to the myocontrol of multi-DOF prosthetic hands. In *Int. Conf. on Intelligent Robots and Systems*, pages 516–521. IEEE, October 2009.
- [Zheng and Qian, 2005] Yu Zheng and Wen-Han Qian. Coping with the grasping uncertainties in force-closure analysis. *Int. J. Rob. Res.*, 24(4):311–327, April 2005.